

EGFR and c-MET Cooperate to Enhance Resistance to PARP Inhibitors in Hepatocellular Carcinoma



Qiong Zhu Dong^{1,2}, Yi Du¹, Hui Li^{1,3}, Chunxiao Liu¹, Yongkun Wei¹, Mei-Kuang Chen^{1,4}, Xixi Zhao¹, Yu-Yi Chu¹, Yufan Qiu¹, Lunxiu Qin², Hirohito Yamaguchi¹, and Mien-Chie Hung^{1,4,5}

Abstract

PARP1 inhibitors (PARPi) are currently used in the clinic for the treatment of ovarian and breast cancers, yet their therapeutic efficacy against hepatocellular carcinoma (HCC) has been disappointing. To ensure therapeutic efficacy of PARPi against HCC, a disease often diagnosed at intermediate to advanced stages with no effective treatment options, it is critical to identify not only biomarkers to predict PARPi resistance but also rational treatments to overcome this. Here, we report that a heterodimer of EGFR and MET interacts with and phosphorylates Y907 of PARP1 in the nucleus, which contributes to

PARPi resistance. Inhibition of both EGFR and MET sensitized HCC cells to PARPi, and both EGFR and MET are known to be overexpressed in HCC. This report provides an explanation for the poor efficacy of PARPi against HCC and suggests combinatorial treatment consisting of EGFR, MET, and PARP inhibitors may be an effective therapeutic strategy in HCC.

Significance: Regulation of PARP by the c-MET and EGFR heterodimer suggests a potentially effective combination therapy to sensitize HCC to PARPi.

Introduction

Liver cancer is the second leading cause of cancer deaths in men worldwide (1). The global incidence of liver cancer is increasing, with a disease-specific death that has doubled over the past two decades (2). Hepatocellular carcinoma (HCC) is the most common form of liver cancer and accounts for 85% to 90% of all primary liver cancers worldwide (3). Although the survival rate for patients with HCC has increased due to the improvement of surgical techniques and perioperative management over the years, the prognosis of patients with HCC remains dismal (3). Among

the treatment options available, small-molecules inhibitors, such as sorafenib and regorafenib that target multiple kinases, are currently approved by the FDA for the treatment of patients with advanced HCC (4, 5). However, both sorafenib and regorafenib only improved the median overall survival in patients with advanced HCC by less than 3 months (4, 5). More recently, the FDA approved nivolumab targeting immune-checkpoint protein programmed death 1 (PD-1) for the treatment of patients with HCC who were previously treated with sorafenib and later developed resistance, but the efficacy of these therapies in HCC is still limited (6). Thus, identifying effective therapeutic strategies for advanced HCC is urgently needed.

The PARP1 enzyme transfers the poly (ADP-ribose) (PAR) chain to various acceptor proteins, such as histone, DNA repair proteins, and PARP1 itself. This process is critical for DNA repair, especially in base excision repair (7, 8). PARP1 inhibitors (PARPi) are considered to be attractive therapeutics for many diseases, including ovarian and breast cancers (9, 10). We recently demonstrated that oxidative DNA damage, such as H₂O₂-induced reactive oxygen species (ROS), activates receptor tyrosine kinase (RTK) MET and promotes its interaction with and phosphorylation of PARP1 at tyrosine 907 (Y907), resulting in PARP activation and PARPi resistance in triple-negative breast cancer (TNBC; ref. 11). Therefore, the combination of PARP1 and MET inhibitors (METi) may provide a promising approach for the treatment of MET-expressing TNBC. To date, several PARPi have been developed and tested in multiple clinical trials (12). For instance, olaparib, rucaparib, and niraparib are approved for the treatment of ovarian cancer, whereas olaparib was recently approved for the treatment of BRCA-mutated breast cancer. However, there have been few clinical trials of PARPi for HCC, and the outcomes have been disappointing (13). Interestingly, MET has been reported to be overexpressed in HCC (14). Here, we sought to delineate the role of phosphorylated Y907 (pY907) by MET in PARPi sensitivity

¹Department of Molecular and Cellular Oncology, The University of Texas MD Anderson Cancer Center, Houston, Texas. ²Department of General Surgery, Huashan Hospital & Cancer Metastasis Institute & Institutes of Biomedical Sciences, Fudan University, Shanghai, China. ³Liver Surgery Department, Liver Cancer Institute, Zhongshan Hospital, Fudan University, Shanghai, China. ⁴Graduate School of Biomedical Sciences, The University of Texas Health Science Center at Houston, Houston, Texas. ⁵Graduate Institute of Biomedical Sciences and Center for Molecular Medicine, China Medical University, Taichung, Taiwan.

Note: Supplementary data for this article are available at Cancer Research Online (<http://cancerres.aacrjournals.org/>).

Current address of M.-C. Hung: Cancer Research Center, Qatar Biomedical Research Institute, College of Science and Engineering, Hamad Bin Khalifa University, Qatar Foundation, Doha, Qatar.

Q. Dong and Y. Du contributed equally to this article.

Corresponding Authors: Mien-Chie Hung, The University of Texas MD Anderson Cancer Center, 1515 Holcombe Boulevard, Unit 108, Houston, TX 77030. Phone: 713-792-3668; Fax: 713-794-3270; E-mail: mhung@mdanderson.org; and Hirohito Yamaguchi, Phone: 713-794-1698; Fax: 713-794-3270; E-mail: hyamaguc@mdanderson.org

doi: 10.1158/0008-5472.CAN-18-1273

©2018 American Association for Cancer Research.

in HCC and unexpectedly discovered the phosphorylation of PARP by the MET and EGFR heterodimer in certain HCC cells. The results suggested that the MET/EGFR heterodimer may serve as biomarkers to stratify patients with HCC for rational combination treatment with PARPi for HCC.

Materials and Methods

HCC tissue samples from patients

A total of 274 patients, who underwent curative surgical resection of HCC as primary treatment at Huashan Hospital, Fudan University (Shanghai, China), were enrolled in this study. Written-informed consent was obtained from all patients. Formalin-fixed and paraffin-embedded tissues from consecutive patients with HCC were used to construct a tissue microarray (TMA) for IHC studies. This study was approved by the Research Ethics Committee of Huashan Hospital, Fudan University, and obtained informed consent at the time of enrollment according to the committee's regulations and the Declaration of Helsinki. The detailed clinicopathologic characteristics of the study participants are presented in Supplementary Table S1.

Cell culture and stable transfectants

All cell lines were obtained from the ATCC and cultured in DMEM/Nutrient Mixture F-12 (DMEM/F12) or RPMI-1640 (Thermo Fisher Scientific) supplemented with 10% (v/v) FCS at 37°C in a humidified incubator containing 5% CO₂. Cell lines were independently validated by short tandem repeat DNA fingerprinting at MD Anderson Cancer Center (Houston, TX), and tests for mycoplasma infection were negative. EGFR (#400015-NIC) knockout cells were established using CRISPR/Cas9 KO plasmids from Santa Cruz Biotechnology. Stable knockdown of MET in HCC cells was performed as described previously (11).

Antibodies and chemicals

Antibodies used in this study are as follows: tubulin (#T5168) and Flag (#F3165) were purchased from Sigma-Aldrich; PARP1 (#sc-7150) for Western blotting from Santa Cruz Biotechnology; PARP1 (#9532) for immunoprecipitation (IP), MET (#8198), phosphorylated MET (#3077), phosphorylated EGFR for IHC (#3777), and EGFR (#4267) from Cell Signaling Technology; and phosphorylated EGFR for Western blotting (#5650), Ki67 (#21700), cleaved caspase-3 (#2302), γ H2AX (#140498), and PAR (#14460) from Abcam; 8-hydroxy-2'-deoxy guanosine (8-OHdG) from Genox Corporation. The mouse phospho-Y907-PARP1 antibody was generated against a phosphorylated synthetic peptide (ADMVSKSAN-Yp-CHTSQGD) at China Medical University as described previously (11). The following inhibitors were used in this study: MET kinase inhibitor crizotinib (#C-7900) was purchased from LC Laboratories; EGFR inhibitor (EGFRi) gefitinib (#S1025) and erlotinib (#S1023) from Selleck Chemicals; PARP inhibitors ABT-888 (veliparib, #CT-A888) and AG014699 (rucaparib, #CT-AG01) from ChemieTek. Hydrogen peroxide (#216763) and sodium arsenite solution (#35000) were obtained from Sigma-Aldrich.

Human phospho-RTK antibody array

The Human Phospho-RTK Array Kit (#ARY003B) was purchased from R&D Systems. Tong/HCC and SK-Hep1 cells were treated with 20 mmol/L H₂O₂ with or without 1 μ mol/L crizotinib for 30 minutes, and cell lysates were incubated with the RTK

array membranes. Array screening was performed according to the manufacturer's protocol. The density of each dot on the membranes was calculated by the GS-800 Calibrated Densitometer (Bio-Rad Laboratories).

IHC staining and evaluation of IHC scores

IHC staining was performed as previously described (11). The tissue specimens were incubated with antibodies against 8-OHdG, EGFR, MET, pY907-PARP1, Ki67, c-caspase-3, γ H2AX, p-EGFR, p-MET, or PAR followed by incubation with biotin-conjugated secondary antibody and avidin-peroxidase, and visualization by aminoethyl carbazole chromogen. Scoring for IHC staining was conducted based on staining intensity and the percentage of positive staining cells. Based on the intensity of staining in section, the intensity was classified into four groups: 3, strong; 2, moderate; 1, weak; and 0, negative. Five fields of cancer cells were randomly selected from each patient for scoring based on the proportion of positively stained cells (0%–100%). The final IHC score was calculated by multiplying the intensity and proportion scores of positive cells. Stained tissue sections were evaluated manually by two independent experienced pathologists without knowledge of other characteristics of the samples.

Western blotting analysis, IP, confocal microscopy analysis, and cellular fractionation

For Western blotting analysis, cell lysates or immunoprecipitates were separated by 8% to 10% SDS-PAGE gels and transferred onto PVDF membranes. The membranes were blocked and incubated with primary antibodies and secondary antibodies. The signals were detected by using Clarity Max Western ECL Blotting Substrates (Bio-Rad). For IP, cell lysates were incubated with 1 μ g of primary antibodies or IgG antibody at 4°C overnight followed by incubation with protein G-agarose beads at 4°C for 1 hour. Protein G-agarose beads were then washed 3 times and subjected to Western blotting analysis. For confocal microscopy analysis, Hep3B cells were grown on chamber slides (Labtek). Cells were then fixed, permeabilized, and incubated with primary antibodies and fluorescence-labeled secondary antibodies. The results were analyzed using Zeiss LSM 710 laser-scanning microscope (Carl Zeiss). The ZEN and AxioVision (Carl Zeiss) and ImageJ software programs (NIH, Bethesda, MD) were used for data analysis. Subcellular fractionation was performed as described previously (15). In brief, cells were homogenized using a Dounce homogenizer in hypotonic buffer, and nuclei were pelleted via centrifugation at 600 \times g for 5 minutes. The remaining pellets were solubilized and sonicated in NETN buffer, and then centrifuged at 16,000 \times g for 5 minutes. The supernatant was collected as the nuclear fraction.

Cell viability assay

Cells were seeded in a 96-well plate (1,500/well). After overnight incubation, cells were treated with the indicated inhibitors for 72 hours. Then cells were incubated in fresh media with 100 μ mol/L resazurin for 1 hour, and cell viability was measured using a fluorescent plate reader at 560_{EX} nm/590_{EM} nm. All experiments were performed in triplicate.

Quantification of drug combination index

Cell growth was measured by cell viability assay. Drug combination studies and their synergy effects were evaluated by the

Chou–Talalay method (16) to calculate the combination index (CI).

Colony formation assay

Cells were seeded in 24-well plates (2,000 cells/well for Hep3B and SK-Hep1; 1,000 cells/well for Tong/HCC) and cultured with or without drugs for 10 days. Cells were then fixed with 3.7% of formaldehyde and stained with crystal violet solution. After taking images of the plates, 0.5% of SDS solution was added to each well, and the plates were incubated for 2 hours at room temperature. The relative densities of cells were then determined by measuring the absorbance of the solution at 570 nm using a microplate reader. The experiments were performed in triplicate.

In vitro kinase assay

MET protein was immunoprecipitated from Hep3B parental and EGFR KO cells washed by cold-PBS 3 times. The immunoprecipitates were resuspended in 500 μ L 1x kinase buffer (#9802, Cell Signaling Technology), with 50 μ L retained for Western blotting. The beads were spun down, and 500 μ mol/L ATP (#9804, Cell Signaling Technology) and 0.5 μ g human recombinant active PARP1 protein (#80501, BPS Bioscience) were added to 20 μ L kinase buffer at 30°C for 30 minutes. The kinase reaction was stopped by heating at 100°C for 5 minutes in SDS loading dye. The samples were subjected to Western blotting to detect phosphorylation of substrate.

Animal studies

All animal experiments were approved by The Animal Care and Use Committee of Fudan University, China. All BALB/c nude mice (4- to 6-week-old male) were obtained from Shanghai Slac Laboratory Animal Co. and fed in a pathogen-free vivarium under standard conditions. Hep3B cells or Huh7 cells (5×10^6) were injected subcutaneously into the flank of nude mice. When tumor volume reached approximately 100 mm³, erlotinib (10 mg/kg), crizotinib (10 mg/kg), and AG014699 (10 mg/kg) were administered orally 5 days per week as single agent or in combination. Tumor growth was monitored with tumor volume, which was calculated as described (17). Tumor samples were collected after final treatment and analyzed by IHC staining.

Statistical analysis

Statistical analyses were performed with SPSS 16.0 for Windows (IBM). The difference between groups was compared using the Student *t* test or one-way ANOVA analysis. Pearson χ^2 test was performed to analyze IHC data. Values are expressed as mean \pm SD. A *P* value < 0.05 was considered statistically significant.

Results

Oxidative DNA damage–induced PARP1 Y907 phosphorylation can be regulated by a kinase other than MET in human HCC tissues

To address whether oxidative DNA damage–mediated MET also increases PARP1 Y907 phosphorylation in HCC, similar to what was observed in TNBC breast cancer (11), we first evaluated the oxidative DNA damage marker 8-OHdG on a human HCC TMA by IHC and found that 8-OHdG level was higher in HCC tumor tissues than in the peritumor tissues (Fig. 1A), indicating oxidative damage is increased in HCC. Next, we examined the levels of oxidative DNA damage marker 8-OHdG and PARP1

pY907 in HCC tumor tissues by IHC staining. The results indicated a significant positive correlation between PARP1 pY907 and 8-OHdG (*P* = 0.008; Fig. 1B), suggesting that similar to TNBC, higher oxidative DNA damage may lead to phosphorylation of PARP1 at Y907 by MET in HCC. Interestingly, although we used the METi, crizotinib, to block the oxidative DNA damage–induced PARP1 pY907 in multiple HCC cell lines by H₂O₂–induced ROS, three different types of responses were observed. In some HCC cell lines, such as SK-Hep1, Tong/HCC, and Hep3B, crizotinib did not block the pY907-PARP1 induced by oxidative DNA damage (Fig. 1C), whereas others, such as Huh-7, PLC/PRF5, HA59T, and HA22T, exhibited similar response to breast cancer cells in which METi blocked the pY907-PARP1 induced by oxidative DNA damage (Fig. 1D; Supplementary Fig. S1A). In other HCC cell lines, oxidative DNA damage did not induce p-Y907-PARP1 (Supplementary Fig. S1B). In the immortalized noncancerous hepatocyte cell line WRL68, although ROS induced MET phosphorylation, which can be blocked by crizotinib, ROS did not induce p-Y907-PARP1 (Fig. 1E). Next, we asked whether other cancer types also have similar responses to oxidative DNA damage and METi. We found that in different cancer types the responses were different. In all the five colon cancer cell lines we tested, METi blocked oxidative DNA damage–induced pY907-PARP1 (Supplementary Fig. S2A). In contrast, 5 of 12 ovarian cell lines responded well to METi (Supplementary Fig. S2A) but not the other seven (Supplementary Fig. S2B). All the three prostate cancer cell lines tested did not respond to METi (Supplementary Fig. S2B). These findings indicated that ROS-induced PARP1 phosphorylation may be cancer type–specific and that PARP1 pY907 may be regulated by another kinase(s) in some HCC cells that do not respond to MET inhibition.

EGFR is involved in PARP1 Y907 phosphorylation

ROS is generally recognized as an activator of RTKs (18). To identify which tyrosine kinases are involved in ROS-induced PARP1 pY907 in those HCC cells nonresponsive to METi, we treated SK-Hep1 and Tong/HCC cells with H₂O₂ with or without crizotinib pretreatment and subjected them to an RTK antibody array analysis (Supplementary Fig. S3A and S3B). The data indicated EGFR as the major kinase activated by H₂O₂ but not blocked by crizotinib (Fig. 2A and B). To further validate the results from the RTK array analysis and determine whether EGFR is involved in the regulation of pY907-PARP1, we treated Hep3B, SK-Hep1, and Tong/HCC cells, which are not sensitive to pY907-PARP1 blockade by the METi under oxidative DNA damage (H₂O₂), in the presence or absence of crizotinib and/or EGFRi gefitinib. Interestingly, compared with pretreatment of single inhibitor, the combination of EGFR and METi depleted H₂O₂–induced pY907-PARP1 most effectively (lane 6 vs. lanes 3, 4, and 5; Fig. 2C; Supplementary Fig. S4). In contrast, we did not observe any changes in PARP1 pY907 after H₂O₂ and kinase inhibitors' treatment in WRL-68, a normal embryonic liver cell line (Fig. 2D). Thus, PARP1 Y907 phosphorylation may be regulated by both EGFR and MET in these HCC cells. To simplify the description, cells in which PARP1 Y907 phosphorylation can be inhibited by the METi alone, such as PLC/PRF5 (similar to breast cancer cells), are referred to as M-type; cells in which inhibition of PARP1 Y907 phosphorylation requires both MET and EGFRi, such as Tong/HCC, SK-Hep1, and Hep3B, are designated as M/E-type.

To validate the significance of EGFR and MET in pY907 in HCC, patient tumor tissues were subjected to IHC staining with EGFR,

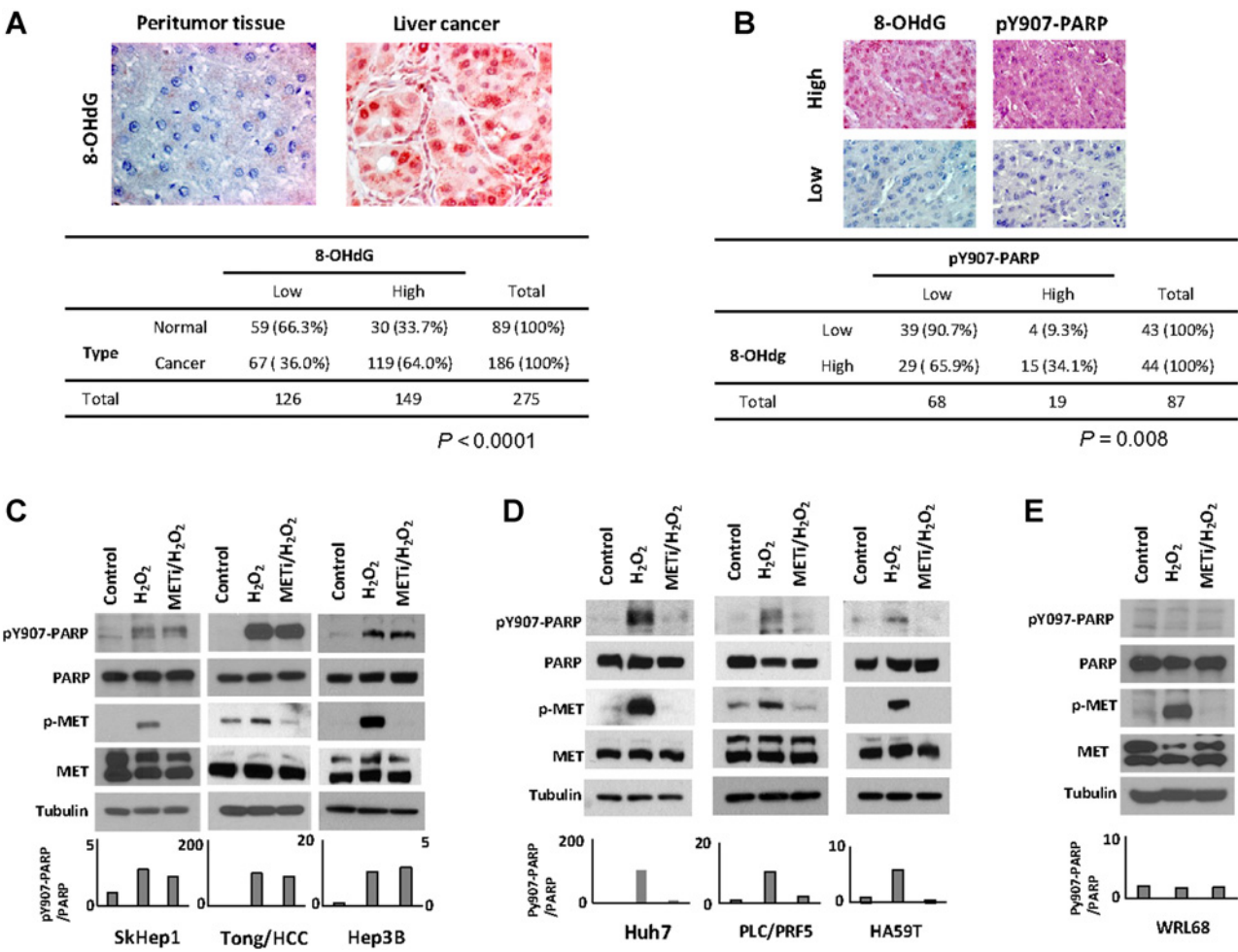


Figure 1. Oxidative stress regulates PARP1 Y907 phosphorylation in liver cancer. **A**, HCC and the peritumor tissues were stained with 8-OHdG antibody. Represented images of IHC staining are shown. **B**, Correlation between pY907 of PARP1 and 8-OHdG in HCC. Representative images of IHC staining are shown. Correlation analyses were performed by the Pearson χ^2 test ($P = 0.008$). **C** and **D**, Various liver cancer cell lines were treated or untreated with 1 $\mu\text{mol/L}$ crizotinib (METi) for 1 hour and further cultured in the presence of 20 mmol/L H₂O₂ for additional 30 minutes. Cells were then lysed and subjected to Western blotting analysis with the indicated antibodies. **E**, WRL68-immortalized noncancerous hepatocyte cells were treated with or without 1 $\mu\text{mol/L}$ crizotinib (METi) for 1 hour and further cultured in the presence of 20 mmol/L H₂O₂ for an additional 30 minutes. Cells were then lysed and subjected to Western blotting analysis with the indicated antibodies.

MET, and pY907 antibodies. EGFR levels closely correlated with MET expression levels in HCC tissues ($P < 0.001$; Fig. 2E). Furthermore, both EGFR and MET exhibited positive correlation with PARP1 pY907 ($P < 0.001$; Fig. 2E), suggesting that EGFR and MET may play a role in pY907 in HCC.

The combined inhibition of EGFR and MET sensitizes HCC cells to PARPi

Because inhibition of both EGFR and MET can suppress PARP1 p-Y907, we asked whether inhibition of both kinase activities sensitizes HCC cell growth to PARPi. To the end, we first treated Hep3B and SK-Hep1 (M/E-type) cells with PARPi and/or kinase inhibitors, and then performed cell proliferation assay to examine the potential synergistic effects (CompuSyn) of triple combination treatment of MET (crizotinib), EGFR (gefitinib), and PARP (AG014699) inhibitors. In Hep3B and SkHep1 cells, triple inhi-

bitors induced synergistic inhibition of cell growth (Fig. 3A; Supplementary Fig. S5A). The values for CI of PARPi with both gefitinib and crizotinib together but not with each inhibitor alone were below 1 (Fig. 3B; Supplementary Fig. S5A), suggesting the synergistically enhanced effects of PARPi, AG014699. As expected, crizotinib alone sensitized M-type PLC/PRF5 cells to PARPi (Supplementary Fig. S5B), indicating PARP1 pY907 is regulated by MET alone in this PLC/PRF5 HCC cell line. To determine whether the inhibitors we used specifically inhibited the enzyme activity in M/E-type cells, we used serial dilution of the inhibitors and examined the activity markers by Western blotting analysis (Supplementary Fig. S6). Gefitinib fully inhibited EGFR phosphorylation at a low concentration (1.5 $\mu\text{mol/L}$). As negative control, FGFR phosphorylation was not inhibited by gefitinib at a high concentration (25 $\mu\text{mol/L}$; Supplementary Fig. S6A). Crizotinib inhibited MET phosphorylation at high concentration

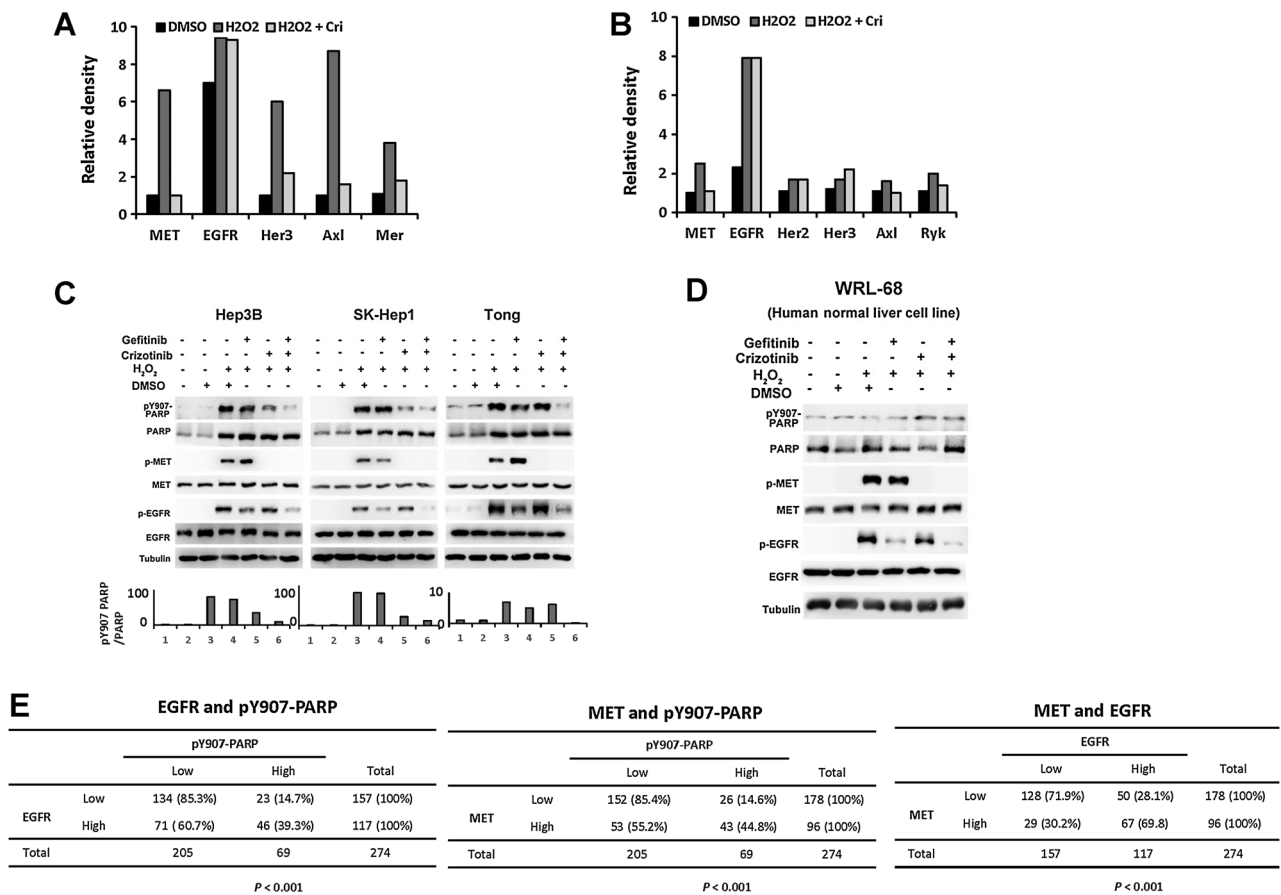
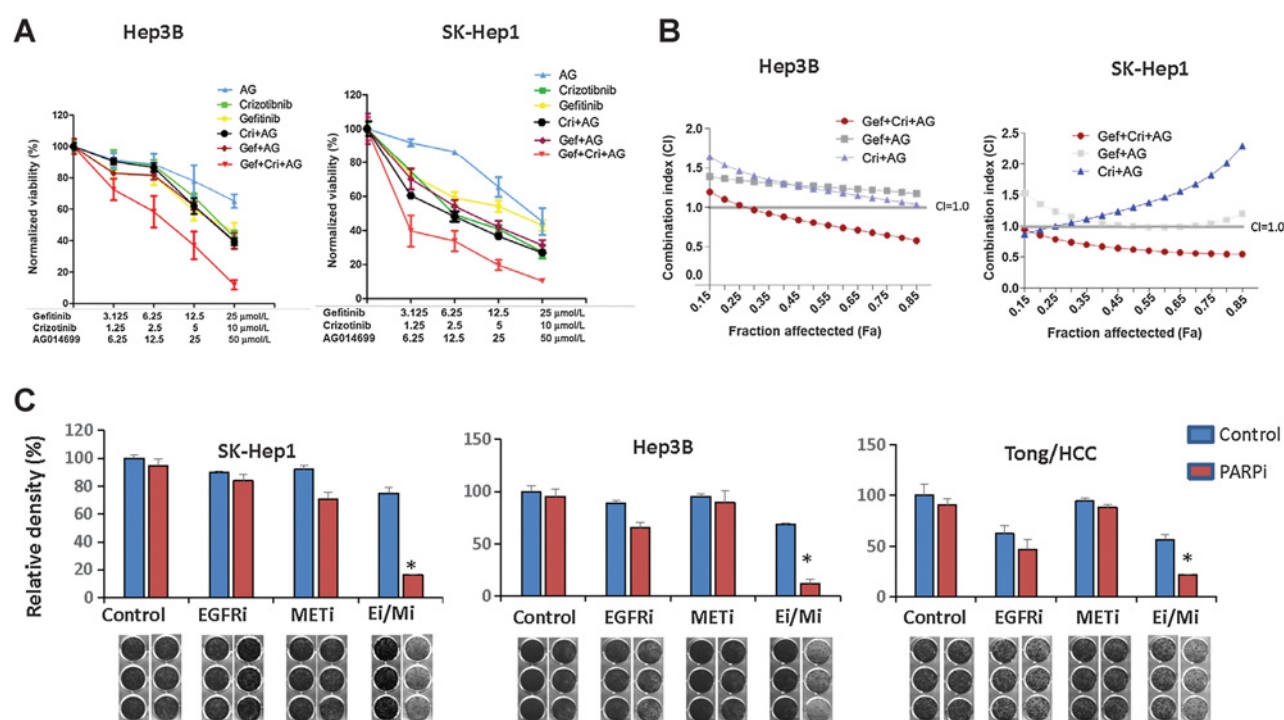


Figure 2. EGFR is the potential kinase that regulates PARP1 Y907 phosphorylation in response to ROS. **A** and **B**, Tong/HCC (**A**) and SK-Hep1 (**B**) cells were treated with 20 mmol/L H₂O₂ with or without 1 μmol/L crizotinib (METi) for 30 minutes and subjected to RTK antibody array. Relative signal intensities are shown. The images of RTK array are shown in Supplementary Fig. S3. **C**, Various liver cancer cells were treated with H₂O₂ with or without 1 μmol/L crizotinib (METi) and/or gefitinib (EGFRi) for 30 minutes and subjected to Western blotting analysis with the indicated antibodies. **D**, WRL68-immortalized noncancerous hepatocyte cells were treated with H₂O₂ with or without 1 μmol/L crizotinib (METi) and/or gefitinib (EGFRi) for 30 minutes and subjected to Western blotting analysis with the indicated antibodies. **E**, Correlation analysis of pY907 of PARP1 and EGFR ($P < 0.001$) or MET ($P < 0.001$) in HCC by Pearson χ^2 test.

(Supplementary Fig. S6B). As negative control, ALK phosphorylation was not inhibited by crizotinib at high concentration (Supplementary Fig. S6B). AG014699 inhibited PARP activity as indicated by the reduced PAR levels (Supplementary Fig. S6C). These results suggested that the M/E-type cells are resistant to METi. We then further examined the effects of inhibition of both EGFR and MET on PARPi by colony formation assay. The results indicated that the combination of gefitinib and crizotinib significantly increased the inhibitory effects of PARPi, but not each kinase inhibitor alone (Fig. 3C).
Next, we compared the effects of the drug combination *in vivo* between M/E-type and M-type cells. First, we treated mice bearing Hep3B (M/E-type) xenograft tumors with the AG014699, erlotinib, crizotinib, or their combination. The three-drug combination induced significantly higher antitumor activity than each drug alone or the combination of AG014699 and crizotinib. The combined treatment of AG014699 and crizotinib did not significantly inhibit tumor growth compared with control or single drug alone (Fig. 4A). The effects of the inhibitors on cell proliferation, apoptosis, and DNA damage were also evaluated by IHC

staining with antibodies against Ki67, cleaved caspase-3, and γ H2AX (Supplementary Fig. S7). Consistent with the above *in vitro* results (Fig. 3), combined treatment of the three inhibitors suppressed cell proliferation much more potently and increased apoptosis and DNA damage compared with each agent alone (Supplementary Fig. S7). In addition, we evaluated the body weight and kidney and liver functions of the mice to determine the toxicity of the three-drug combination and did not observe any significant differences between the different treatment groups (Fig. 4B and C), indicating that each drug or their combination was well tolerated. Furthermore, we also compared the effects of three inhibitors on the activity of EGFR, MET, and PARP by IHC staining in tumor tissues from mice with subcutaneous Hep3B implantation (Supplementary Fig. S8). Erlotinib and crizotinib significantly inhibited p-EGFR and p-MET, respectively. AG014699 significantly inhibited PARP activity as indicated by reduced PAR level. As expected, the combination of the three inhibitors can also significantly inhibit the activity of EGFR, MET, and PARP. Contrary to M/E type, the combined treatment of AG014699 and crizotinib demonstrated significant antitumor

**Figure 3.**

The combination of EGFR and METi sensitizes some HCC cells to PARPi. **A** and **B**, Hep3B and SK-Hep1 cells were treated with the indicated concentration of EGFRi (Gef, gefitinib), METi (Cri, crizotinib), and PARPi (AG, AG014699) for 3 days. Cells were then subjected to MTT assay to determine cell viability (**A**) and CI determined (**B**). **C**, Hep3B, SK-Hep1, and Tong/HCC cells were subjected to colony formation assay. Cells were cultured in the presence of METi (Cri, crizotinib), EGFRi (Erl, erlotinib), and/or PARPi (Ola, olaparib). The drug concentrations used for the colony formation assay are as follows: SK-Hep1: Ola 1.25 μmol/L, Erl 1.25 μmol/L, and Cri 0.25 μmol/L; Hep3B: Ola 1.25 μmol/L, Erl 0.625 μmol/L, and Cri 0.25 μmol/L; Tong: Ola 2.5 μmol/L, Erl 0.5 μmol/L, and Cri 0.5 μmol/L. Top, relative colony densities shown. *, $P < 0.01$, three-combination vs. two-combination drug treatment.

activity in the M-type liver cancer Huh7 xenograft tumor models (Fig. 4D). Mice that received the combination treatment did not show any significant changes in body weight (Fig. 4E) or elevation in liver enzyme (ALT and AST), kidney toxicity marker, or blood urea nitrogen (Fig. 4F). Together, these findings suggested that PARPi may be combined with both EGFR and METi in the clinic as a potential therapeutic strategy for liver cancer.

EGFR cooperates with MET to regulate PARP1

On the basis of the above findings, we speculated that EGFR interacts with MET to induce PARP1 phosphorylation. To this end, we carried out co-IP assay to first examine the interaction between EGFR and MET. As expected, EGFR interacted with MET in both Hep3B and SK-Hep1 cells (Supplementary Fig. S9). Interestingly, although we did not observe any differences in EGFR and MET expression between M/E-type and M-type liver cancer cell lines, the interaction between EGFR and MET was stronger in the M/E type than in the M type (Supplementary Fig. S10). We previously showed that MET translocates into the nucleus in response to ROS and interacts with and phosphorylates PARP1 (11). Thus, we determined the localization of EGFR and MET after oxidative DNA damage by subcellular fractionation and Western blotting analysis. We found that EGFR translocated into the nucleus in response to ROS, whereas MET was localized in both the nucleus and cytoplasm independently of oxidative DNA damage in the M/E-type HCC (Fig. 5A and B). Moreover, MET

nuclear localization was not altered by treatment of crizotinib. Similarly, the ROS-induced nuclear EGFR also remained in the nucleus after gefitinib treatment. Confocal microscopy further validated those results (Fig. 5C). In contrast, in the M-type liver cancer cells, such as PLC/PRF5 and Huh-7, ROS induced nuclear translocation of MET similar to that observed in breast cancer cells (Supplementary Fig. S11; ref. 11). Given that EGFR or MET activates PARP1 in response to ROS, we speculated that MET and EGFR may physically interact with PARP1. Indeed, our data indicated that EGFR forms a complex with MET and PARP1, which was not blocked by either kinase inhibitor alone (Fig. 5D and E). Interestingly, the combination of EGFR and METi abrogated EGFR/MET, EGFR/PARP1, and MET/PARP1 complexes (Fig. 5F). These results are consistent with those showing that pY907-PARP was only inhibited when treated with both gefitinib and crizotinib. Taken together, these results suggest that in the M/E-type HCC, EGFR translocates to the nucleus and forms a complex with MET and phosphorylates PARP1 in response to oxidative stress, e.g., H_2O_2 .

EGFR and MET heterodimer interacts with and phosphorylates PARP1

To further investigate whether EGFR and MET interaction regulates PARP1, we first knocked out EGFR by using CRSPR-Cas9 system in Hep3B and SK-Hep1 cells. MET and PARP1 interaction in parental and EGFR-knockout (KO) cells after

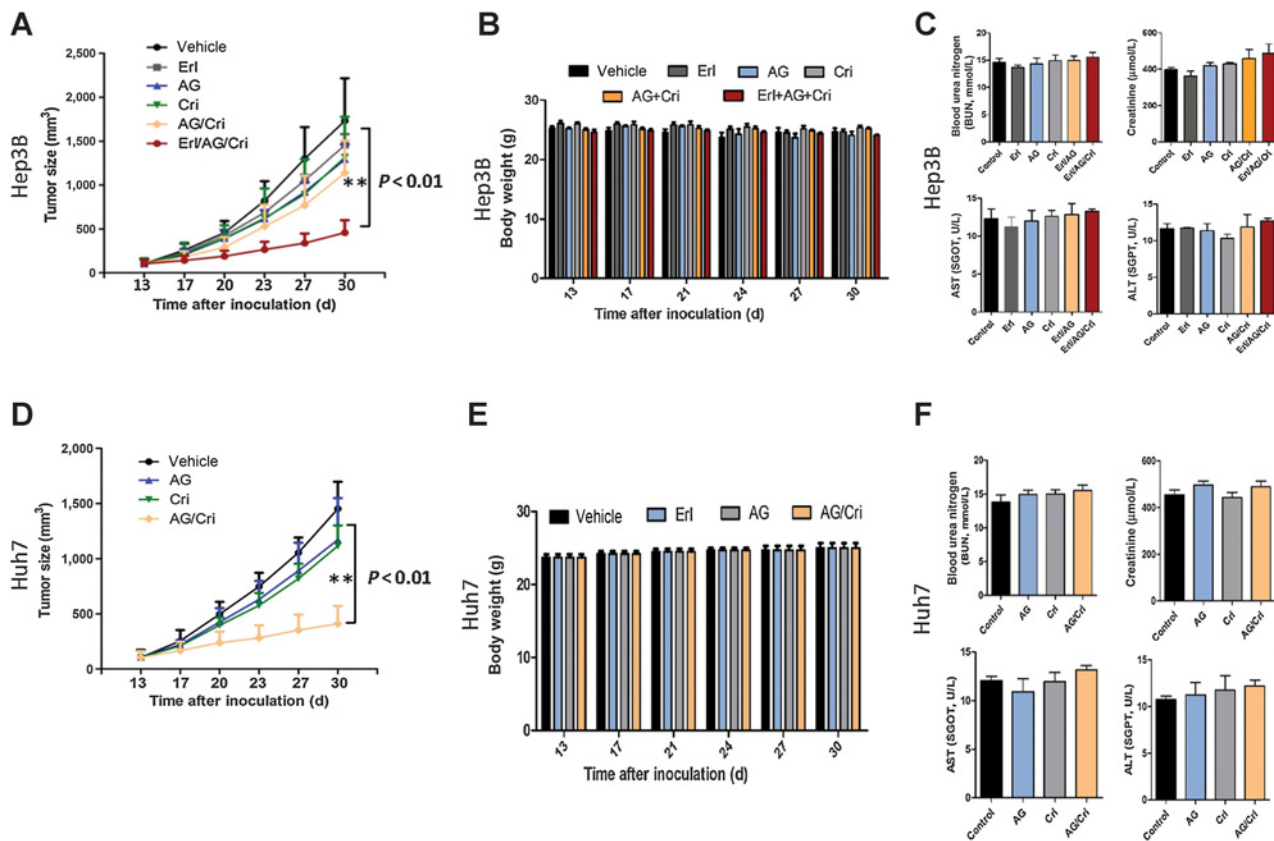


Figure 4.

Combination of EGFRi and METi sensitizes Hep3B xenograph tumors to PARPi. **A**, Tumor growth curves of subcutaneous implantation models of Hep3B cells are shown. When tumor volume reached approximately 100 mm³, mice were treated with inhibitor against EGFR (Erl, erlotinib, 10 mg/kg), MET (Cri, crizotinib, 10 mg/kg), PARP (AG, AG014699, 10 mg/kg), or their combination. For the Hep3B xenograph tumor model, the average body weight of mice during treatment (**B**) and the effects of the indicated drugs on liver and kidney function (**C**) are shown. **D**, Tumor growth curves of subcutaneous implantation models of Huh7 cells are shown. When tumor volume reached approximately 100 mm³, the mice were then treated with inhibitor against MET (Cri, crizotinib, 10 mg/kg), PARP (AG, AG014699, 10 mg/kg), or their combination. For the Huh7 xenograph tumor model, the average body weight of mice during treatment (**E**) and the effects of the indicated drugs on liver and kidney function (**F**) are shown. AST, aspartate aminotransferase; ALT, alanine transaminase. **, $P < 0.01$.

H₂O₂ treatment was determined by co-IP analysis. The result showed that MET and PARP1 interaction was only detected in parental Hep3B and SK-Hep1 cells but not in EGFR-KO cells (Fig. 6A; Supplementary Figs. S12 and S13), indicating that MET–PARP1 interaction requires EGFR. Moreover, the results indicated diminished MET–PARP1 interaction in the absence of EGFR-reduced pY907-PARP1 (Fig. 6A). In addition, we treated Hep3B control and MET-knockdown cells with H₂O₂ and then examined the EGFR–PARP1 interaction. Similarly, EGFR–PARP1 interaction and PARP1 pY907 were abrogated in MET-knockdown cells (Fig. 6B). These results suggested that EGFR and MET form a heterodimer, which is enhanced by oxidative DNA damage, and the EGFR/MET complex interacts with PARP1 in the M/E-type HCC.

Next, we performed the immunocomplex kinase assay of MET with PARP1 protein as a substrate. MET protein purified from Hep3B parental cells demonstrated kinase activity toward purified PARP protein, whereas MET protein from the EGFR KO cells had much lower kinase activity toward purified PARP protein (Fig. 6C), suggesting EGFR is required for MET to phosphorylate

PARP1 Y907 as the EGFR/MET heterodimer likely activates MET (Fig. 6C).

On the basis of these findings, we proposed a working model (Fig. 6D). In M/E type of HCC cells, EGFR translocates into the nucleus in response to oxidative DNA damage, whereas some MET proteins remain localized in the nucleus. Following exposure to oxidative DNA damage, EGFR forms a heterodimer with MET, which then interacts with and phosphorylates MET to activate its kinase activity for subsequent phosphorylation of PARP1 at Y907 in the nucleus. The EGFR/MET heterodimer formation and subsequent interaction with and phosphorylation of PARP are not affected by EGFR or METi alone under oxidative DNA damage. However, inhibition of the kinase activity of both EGFR and MET is needed to prevent their heterodimer formation (Fig. 5F). Together, our data showed that only one of the protein's kinase activity (EGFR or MET) is required for the heterodimer to interact with PARP1 and sufficient to induce PARP Y907 phosphorylation, leading to PARPi resistance. Thus, simultaneous inhibition of both EGFR and MET is a potentially efficient approach to overcome resistance to PARP inhibitors in the M/E-type HCC.

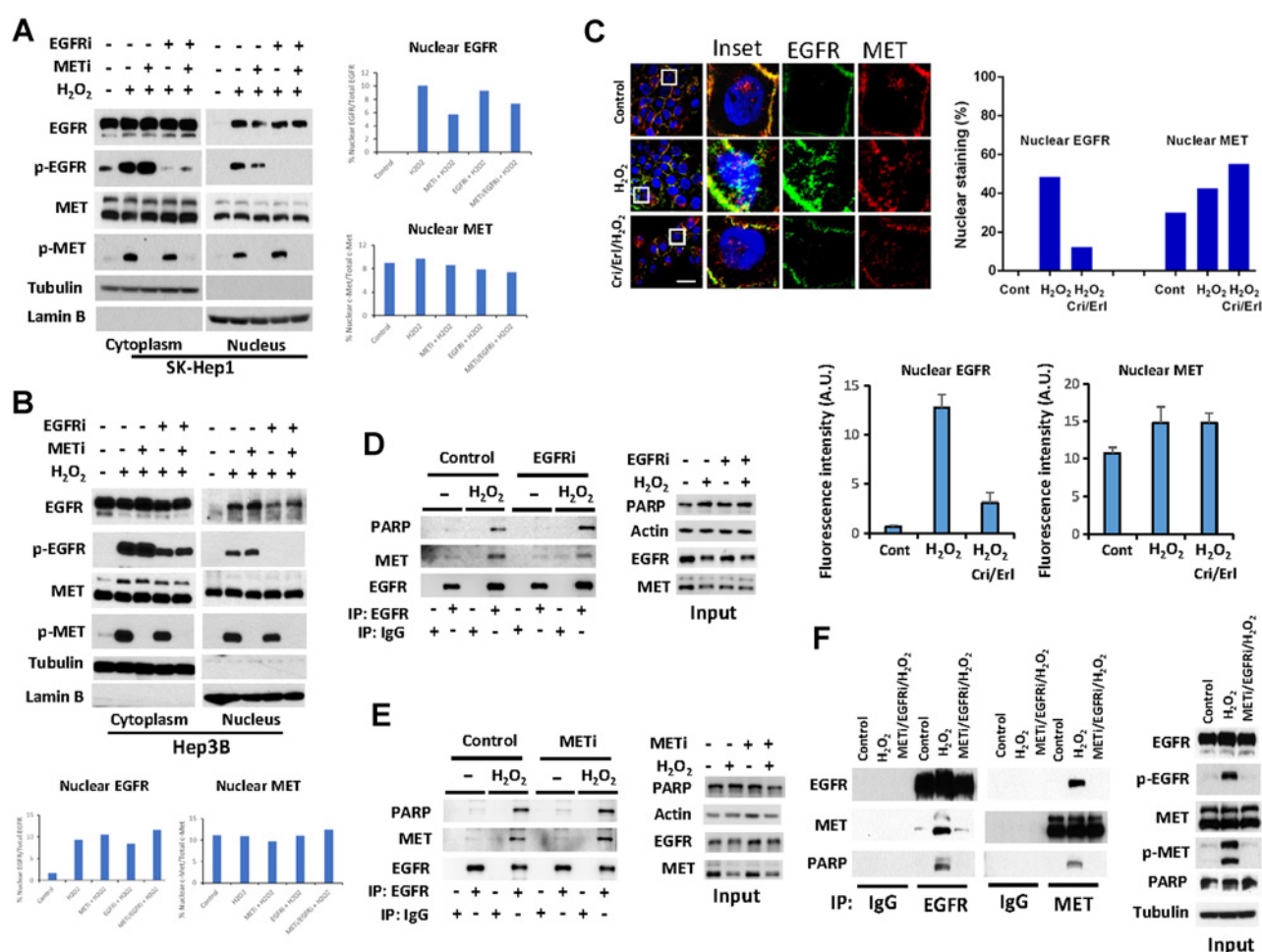


Figure 5.

Regulation of the interaction of EGFR and MET with PARP1. **A** and **B**, SK-Hep1 (**A**) and Hep3B (**B**) cells were treated with H₂O₂ in the presence or absence of EGFRi (erlotinib) and/or METi (crizotinib) for 30 minutes and subjected to subcellular fractionation, followed by Western blotting analysis with the indicated antibodies. LaminB was used as a nuclear marker, and tubulin and calregulin as cytoplasmic markers. **C**, Hep3B cells were treated with 20 mmol/L H₂O₂ in the presence or absence of EGFRi (erlotinib) and METi (crizotinib) for 30 minutes, and fixed and stained with EGFR and MET antibodies. The fluorescence signals were analyzed by using confocal microscopy. The fluorescence intensities of EGFR and MET signals in the nucleus from randomly selected 30 cells were quantified. The percentage of nuclear staining of EGFR and MET was also quantified. Scale bar, 20 μ m. **D**, Hep3B cells were treated with H₂O₂ in the presence or absence of EGFRi (erlotinib). The cells were then subjected to IP with EGFR antibody, followed by Western blotting analysis with the indicated antibodies. **E**, Hep3B cells were treated with H₂O₂ in the presence or absence of METi (crizotinib). The cells were then subjected to IP with EGFR antibody, followed by Western blotting analysis with the indicated antibodies. **F**, Hep3B cells were treated with H₂O₂ in the presence or absence of the combination of EGFRi (erlotinib) and METi (crizotinib). The cells were then subjected to IP with EGFR or MET antibody, followed by Western blotting analysis with the indicated antibodies.

Discussion

There are currently no effective targeted therapies for the advanced HCC, which is the major form of liver cancer (19). For instance, the multikinase inhibitor sorafenib exhibits only moderate overall therapeutic efficacy (20). Future treatment approaches to improve the therapeutic efficacy in patients with HCC is expected to consist of combined targeted therapies based on the molecular classification of each patient. We previously reported that PARP1 is phosphorylated at Y907 by MET, and this phosphorylation increases PARP activity and reduces its affinity to PARPi, resulting in PARPi resistance in TNBC (11). In the current study, we investigated the role of PARP1 Y907 phosphorylation in PARPi resistance in HCC and identified a mechanism regulated by EGFR and MET.

PARP inhibitors have been evaluated in clinical trials for many cancer types (21–23). A recent study demonstrated a high response rate among patients with advanced prostate cancer harboring defects in DNA-repair genes treated with PARP inhibitor olaparib (24). Our recent study demonstrated that combining MET and PARPi produced a synergistic effect to suppress cancer cell growth in TNBC (11). By expanding our findings in breast cancer to HCC, our results indicated that PARP1 Y907 is also phosphorylated in this disease. Interestingly, however, METi did not block the pY907-PARP1 induced by H₂O₂ in a subset of HCC. Indeed, we found that EGFR forms a complex with MET for the phosphorylation of PARP1 at Y907. Compared with single inhibitor alone, the combined treatment of EGFR and METi potently

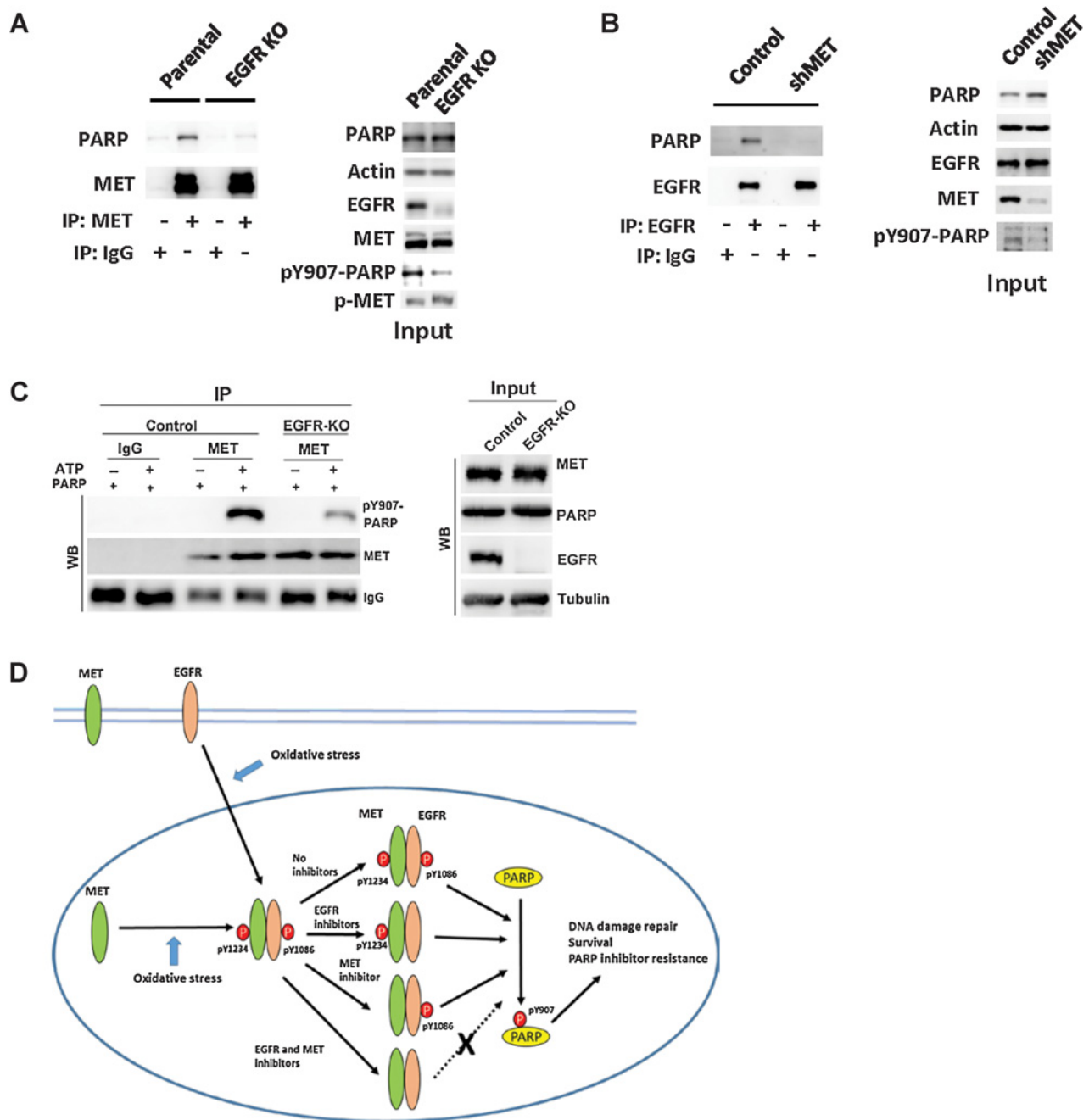


Figure 6.

EGFR requires MET and vice versa for its interaction with PARP1. **A**, Hep3B parental and EGFR knockout cells were treated with H_2O_2 for 30 minutes and subjected to IP with MET antibody, followed by Western blotting analysis with the indicated antibodies. **B**, Hep3B control and MET knockdown cells were treated with H_2O_2 for 30 minutes and subjected to IP with the EGFR antibody, followed by Western blotting analysis with the indicated antibodies. **C**, MET protein was immunoprecipitated from Hep3B parental and EGFR KO cells, and subjected to *in vitro* kinase assay using purified PARP protein. **D**, A proposed model of EGFR and MET-mediated PARP inhibitor resistance in liver cancer. In some liver cancer cells, EGFR translocates to the nucleus in response to oxidative stress, whereas some portion of MET consistently localizes in the nucleus. After cells are exposed to oxidative stress, EGFR forms a heterodimer with MET in the nucleus. Inhibition of EGFR or MET activity does not prevent heterodimerization of MET and EGFR. The EGFR/MET complex interacts with and phosphorylates PARP1 in response to oxidative stress. Simultaneous inhibition of both EGFR and MET is required to overcome PARP inhibitor resistance in some types of liver cancer.

depleted H_2O_2 -induced pY907-PARP1. Moreover, the combined treatment of EGFR, MET, and PARP inhibitors effectively reduced tumor growth. Importantly, the combination of EGFR and METi sensitized M/E-type HCC cells to PARPi, suggesting simultaneous

inhibition of both EGFR and MET is required to overcome PARPi resistance in some types of HCC.

A growing number of studies have investigated the molecular mechanisms underlying intrinsic and acquired resistance to

PARPi (25, 26). Inhibition of NHEJ core proteins, such as the loss of 53BP1 protein, has been shown to contribute to the development of PARPi resistance by restoring HR activity (27). A deficiency in other crucial NHEJ players, Ku70/80 and DNA-PK, also plays a role in PARPi resistance in BRCA1-deficient cells (28). HOXA9 has also been shown to contribute to PARPi resistance of mixed-lineage leukemia through upregulation of HR genes (29). We previously reported that MET-mediated PARP1 phosphorylation is involved in PARPi resistance (11). The crosstalk between RTKs and their direct binding to members of other RTK families are critical during tumor progression. The current study revealed a molecular mechanism underlying PARPi resistance through EGFR/MET heterodimer-mediated phosphorylation of PARP1 in response to oxidative DNA damage even in the presence of inhibitor against EGFR or MET, suggesting the combination of MET and EGFRi is required to induce a synergistic cell killing effect in this type of HCC. In addition, previous study reported that tyrosine kinase inhibitors can inhibit the nuclear translocation of EGFR (30). We also found gefitinib treatment reduced nuclear EGFR in Hep3B cells. However, nuclear EGFR has no change by gefitinib treatment in SK-Hep1 cells. There may be some cell type specific for the effects of gefitinib on the nuclear translocation of EGFR.

For patients with HCC whose tumors express MET but not EGFR, MET-mediated phosphorylation of PARP1 can be blocked by METi plus PARPi (similar to breast cancer). In contrast, for patients with HCC whose tumors express both EGFR and MET, a three-drug combination, e.g., PARPi–METi–EGFRi, may be required. EGFR and MET are overexpressed in 40% to 70% and 50% to 70% of HCC, respectively (14, 31, 32). Considering that most HCC express EGFR, MET, or both, we speculated that a common subset of patients with HCC can be molecularly stratified for treatment, characterized by high expression of EGFR, MET, or both using PARP1 Y907 phosphorylation and MET/EGFR expression as biomarkers to guide the combinational treatment of PARPi and MET/EGFRi. Patients with HCC that overexpress EGFR

or MET may also benefit from this combination therapy. It would be of interest to determine whether this approach could be applied to other cancer types involving PARP1/EGFR/MET overexpression.

Disclosure of Potential Conflicts of Interest

No potential conflicts of interest were disclosed.

Authors' Contributions

Conception and design: Y. Du, H. Yamaguchi

Development of methodology: Q. Dong, Y. Du, H. Li

Acquisition of data (provided animals, acquired and managed patients, provided facilities, etc.): Q. Dong, Y. Du, H. Li, M.-K. Chen, L. Qin, H. Yamaguchi

Analysis and interpretation of data (e.g., statistical analysis, biostatistics, computational analysis): Q. Dong, Y. Du, C. Liu, Y. Wei, M.-K. Chen, H. Yamaguchi, M.-C. Hung

Writing, review, and/or revision of the manuscript: Q. Dong, Y. Du, Y. Wei, H. Yamaguchi, M.-C. Hung

Administrative, technical, or material support (i.e., reporting or organizing data, constructing databases): Q. Dong, C. Liu, X. Zhao, Y.-Y. Chu, Y. Qiu

Study supervision: M.-C. Hung

Acknowledgments

This study was supported by the following: NIH (CCSG CA016672, R01 CA211615, and U01 CA201777); Cancer Prevention and Research Institutes of Texas (RP160710); The University of Texas MD Anderson-China Medical University and Hospital Sister Institution Fund (to M.-C. Hung); Ministry of Health and Welfare, China Medical University Hospital Cancer Research Center of Excellence (MOHW107-TDU-B-212-114024 and MOHW107-TDU-B-212-112015); Center for Biological Pathways; and the National Key Research and Development Program of China (2017YFC1308604).

The costs of publication of this article were defrayed in part by the payment of page charges. This article must therefore be hereby marked *advertisement* in accordance with 18 U.S.C. Section 1734 solely to indicate this fact.

Received April 25, 2018; revised October 12, 2018; accepted December 14, 2018; published first December 20, 2018.

References

- Torre LA, Bray F, Siegel RL, Ferlay J, Lortet-Tieulent J, Jemal A. Global cancer statistics, 2012. *CA Cancer J Clin* 2015;65:87–108.
- Siegel RL, Miller KD, Jemal A. Cancer statistics, 2016. *CA Cancer J Clin* 2016;66:7–30.
- Llovet JM, Zucman-Rossi J, Pikarsky E, Sangro B, Schwartz M, Sherman M, et al. Hepatocellular carcinoma. *Nat Rev Dis Primers* 2016;2:16018.
- Llovet JM, Ricci S, Mazzaferro V, Hilgard P, Gane E, Blanc JF, et al. Sorafenib in advanced hepatocellular carcinoma. *N Engl J Med* 2008;359:378–90.
- Bruix J, Qin S, Merle P, Granito A, Huang YH, Bodoky G, et al. Regorafenib for patients with hepatocellular carcinoma who progressed on sorafenib treatment (RESORCE): a randomised, double-blind, placebo-controlled, phase 3 trial. *Lancet* 2017;389:56–66.
- Zhu YJ, Zheng B, Wang HY, Chen L. New knowledge of the mechanisms of sorafenib resistance in liver cancer. *Acta Pharmacol Sin* 2017;38:614–22.
- Schreiber V, Dantzer F, Ame JC, de Murcia G. Poly(ADP-ribose): novel functions for an old molecule. *Nat Rev Mol Cell Biol* 2006;7:517–28.
- Jayle M, Curtin NJ. The role of PARP in DNA repair and its therapeutic exploitation. *Br J Cancer* 2011;105:1114–22.
- Feng FY, de Bono JS, Rubin MA, Knudsen KE. Chromatin to clinic: the molecular rationale for PARP1 inhibitor function. *Mol Cell* 2015;58:925–34.
- Sonnenblick A, de Azambuja E, Azim HA Jr, Piccart M. An update on PARP inhibitors—moving to the adjuvant setting. *Nat Rev Clin Oncol* 2015;12:27–41.
- Du Y, Yamaguchi H, Wei Y, Hsu JL, Wang HL, Hsu YH, et al. Blocking c-Met-mediated PARP1 phosphorylation enhances anti-tumor effects of PARP inhibitors. *Nat Med* 2016;22:194–201.
- Buege M, Mahajan PB. Clinical trials of poly(ADP-Ribose) polymerase inhibitors for cancer therapy: a review. *Rev Recent Clin Trials* 2015;10:326–39.
- Gabrielson A, Tesfaye AA, Marshall JL, Pishvaian MJ, Smaglo B, Jha R, et al. Phase II study of temozolomide and veliparib combination therapy for sorafenib-refractory advanced hepatocellular carcinoma. *Cancer Chemother Pharmacol* 2015;76:1073–9.
- Giordano S, Columbano A. Met as a therapeutic target in HCC: facts and hopes. *J Hepatol* 2014;60:442–52.
- Du Y, Shen J, Hsu JL, Han Z, Hsu MC, Yang CC, et al. Syntaxin 6-mediated Golgi translocation plays an important role in nuclear functions of EGFR through microtubule-dependent trafficking. *Oncogene* 2014;33:756–70.
- Chou TC. Drug combination studies and their synergy quantification using the Chou-Talalay method. *Cancer Res* 2010;70:440–6.
- Wang L, Tang ZY, Qin LX, Wu XF, Sun HC, Xue Q, et al. High-dose and long-term therapy with interferon- α inhibits tumor growth and recurrence in nude mice bearing human hepatocellular carcinoma xenografts with high metastatic potential. *Hepatology* 2000;32:43–8.
- Chiarugi P, Cirri P. Redox regulation of protein tyrosine phosphatases during receptor tyrosine kinase signal transduction. *Trends Biochem Sci* 2003;28:509–14.

19. Llovet JM, Villanueva A, Lachenmayer A, Finn RS. Advances in targeted therapies for hepatocellular carcinoma in the genomic era. *Nat Rev Clin Oncol* 2015;12:436.
20. Ray EM, Sanoff HK. Optimal therapy for patients with hepatocellular carcinoma and resistance or intolerance to sorafenib: challenges and solutions. *J Hepatocell Carcinoma* 2017;4:131–8.
21. Ramalingam SS, Blais N, Mazieres J, Reck M, Jones CM, Juhasz E, et al. Randomized, placebo-controlled, phase ii study of veliparib in combination with carboplatin and paclitaxel for advanced/metastatic non-small cell lung cancer. *Clin Cancer Res* 2017;23:1937–44.
22. Swisher EM, Lin KK, Oza AM, Scott CL, Giordano H, Sun J, et al. Rucaparib in relapsed, platinum-sensitive high-grade ovarian carcinoma (ARIEL2 Part 1): an international, multicentre, open-label, phase 2 trial. *Lancet Oncol* 2017;18:75–87.
23. Gelmon KA, Tischkowitz M, Mackay H, Swenerton K, Robidoux A, Tonkin K, et al. Olaparib in patients with recurrent high-grade serous or poorly differentiated ovarian carcinoma or triple-negative breast cancer: a phase 2, multicentre, open-label, non-randomised study. *Lancet Oncol* 2011;12:852–61.
24. Mateo J, Carreira S, Sandhu S, Miranda S, Mossop H, Perez-Lopez R, et al. DNA-repair defects and olaparib in metastatic prostate cancer. *N Engl J Med* 2015;373:1697–708.
25. Fojo T, Bates S. Mechanisms of resistance to PARP inhibitors—three and counting. *Cancer Discov* 2013;3:20–3.
26. Rouleau M, Patel A, Hendzel MJ, Kaufmann SH, Poirier GG. PARP inhibition: PARP1 and beyond. *Nat Rev Cancer* 2010;10:293–301.
27. Bunting SF, Callen E, Wong N, Chen HT, Polato F, Gunn A, et al. 53BP1 inhibits homologous recombination in Brca1-deficient cells by blocking resection of DNA breaks. *Cell* 2010;141:243–54.
28. Patel AG, Sarkaria JN, Kaufmann SH. Nonhomologous end joining drives poly(ADP-ribose) polymerase (PARP) inhibitor lethality in homologous recombination-deficient cells. *Proc Natl Acad Sci U S A* 2011;108:3406–11.
29. Esposito MT, Zhao L, Fung TK, Rane JK, Wilson A, Martin N, et al. Synthetic lethal targeting of oncogenic transcription factors in acute leukemia by PARP inhibitors. *Nat Med* 2015;21:1481–90.
30. Kim HP, Yoon YK, Kim JW, Han SW, Hur HS, Park J, et al. Lapatinib, a dual EGFR and HER2 tyrosine kinase inhibitor, downregulates thymidylate synthase by inhibiting the nuclear translocation of EGFR and HER2. *PLoS One* 2009;4:e5933.
31. Ito Y, Takeda T, Sakon M, Tsujimoto M, Higashiyama S, Noda K, et al. Expression and clinical significance of erb-B receptor family in hepatocellular carcinoma. *Br J Cancer* 2001;84:1377–83.
32. Buckley AF, Burgart LJ, Sahai V, Kakar S. Epidermal growth factor receptor expression and gene copy number in conventional hepatocellular carcinoma. *Am J Clin Pathol* 2008;129:245–51.